GEOPHYSICS, VOL. 64, NO. 2 (MARCH-APRIL 1999); P. 378–385, 6 FIGS.

Airborne resistivity data leveling

Haoping Huang* and Douglas C. Fraser*

ABSTRACT

Helicopter-borne frequency-domain electromagnetic (EM) data are used routinely to produce resistivity maps for geologic mapping, mineral exploration, and environmental investigations. The integrity of the resistivity data depends in large part on the leveling procedures. Poor resistivity leveling procedures may, in fact, generate false features as well as eliminate real ones.

Resistivity leveling is performed on gridded data obtained by transformation of the leveled EM channel data. The leveling of EM channel data is often imperfect, which is why the resistivity grids need to be leveled. We present techniques for removing the various types of resistivity leveling errors which may exist. A semi-automated leveling technique uses pseudo tie-lines to remove the broad flight-based leveling errors and any high-magnitude line-based errors. An automated leveling technique employs a combination of 1-D and 2-D nonlinear filters to reject the rest of the leveling errors including both long-and short-wavelength leveling errors. These methods have proven to be useful for DIGHEM helicopter EM survey data. However, caution needs to be exercised when using the automated technique because it cannot distinguish between geological features parallel to the flight lines and leveling errors of the same wavelength.

Resistivity leveling is not totally objective since there are no absolutes to the measured frequency-domain EM data. The fundamental integrity of the EM data depends on calibration and the estimate of the EM zero levels. Zero level errors can be troublesome because there is no means by which the primary field can be determined absolutely and therefore subtracted to yield an absolute measure of the earth's response. The transform of incorrectly zero-leveled EM channels will yield resistivity leveling errors. Although resistivity grids can be leveled empirically to provide an esthetically pleasing map, this is insufficient because the leveling must also be consistent across all frequencies to allow resistivity to be portrayed in section. Generally, when the resistivity looks correct in plan and section, it is assumed to be correct.

INTRODUCTION

Airborne resistivity mapping was first introduced to common usage with the DIGHEM helicopter-borne frequency-domain electromagnetic (EM) system approximately 20 years ago (Fraser, 1978), and is now an accepted method of electrical mapping. The DIGHEM resistivity technique has been used for the location of uranium mineralization (Hasegawa et al., 1990), gold (Taylor, 1990), and diamondiferous kimberlites (James, 1992), and for many nonmining applications such as ocean depth mapping (Won and Smits, 1986), groundwater prospecting (Sengpiel, 1986), geothermal exploration (Hoover and Pierce, 1986), and geological mapping for a variety of purposes including the siting of nuclear power reactors (Deletie and Lakshmanan, 1986) and the disposal of nuclear waste (Soonawala and Hayles, 1986). Airborne resistivity mapping has also been performed by fixed-wing time-domain systems (Dyck et al., 1974; Becker, 1988).

Various models and methods may be used to transform the EM data to a half-space (Huang and Fraser, 1996) or invert it to a layered earth (Fitterman and Deszcz-Pan, 1998). A large dynamic range in resistivities must be capable of being handled because frequencies in helicopter EM systems may range from 200 to 200 000 Hz.

Well-leveled EM data are required to yield resistivity data of the integrity needed for many of the applications listed above. In producing maps and sections of apparent resistivity, the EM data need to be correctly leveled from one frequency to the next, as well as leveled correctly for a given single frequency across the entire map. Having leveled the EM data and computed the resistivity, the resistivity may then need leveling

Published on Geophysics Online October 8, 1998. Manuscript received by the Editor April 4, 1997; revised manuscript received May 14, 1998.
*Geoterrex-Dighem, Unit 2, 2270 Argentia Road, Mississauga, Ontario L5N 6A6, Canada. E-mail: haoping.huang@dighem.com; 105421.2020@compuserve.com (for D. Fraser).

much as magnetics may need leveling to remove a variety of problems.

Helicopter-borne resistivity mapping differs from airborne magnetic mapping in the difficulty of obtaining well-leveled grid images that maintain the integrity of the EM data. The conventional tie-line leveling used for magnetic data is generally not very useful for resistivity leveling because of the rapid changes to the computed resistivity resulting from low-level flying over areas with highly variable conductivity. Also, nonlinear line-based leveling errors may exist, again mitigating against the effectiveness of tie-line leveling.

This paper describes the nature of the resistivity leveling problems encountered in helicopter EM surveys and the techniques used by us to overcome them. There is a paucity of references on airborne resistivity leveling as the subject falls within the "tricks of the trade" of geophysical contractors.

AIRBORNE RESISTIVITY MAPPING

Helicopter EM systems

Helicopter EM systems comprise a "bird" or sensor containing one or more pairs of transmitting and receiving coils (Fraser, 1979). The separation between the rigidly mounted transmitting and receiving coils of a coil-pair typically ranges between 4 and 8 m. The EM bird is towed beneath the helicopter by a cable 30–50 m long. This is a sufficient distance to render the metal of the helicopter virtually undetectable by the EM system.

The receiving coil measures the voltage induced by the primary field from the transmitting coil and by the secondary field from the earth, although much of the primary field is bucked out by various means to preserve dynamic range. The secondary field is typically somewhat out of phase with the primary field, and so two channels of EM information are recorded, often called inphase and quadrature. The unit of measurement is the ratio of the secondary field intensity to the primary field intensity, times 1 000 000, called parts per million (ppm).

Zero levels of EM data

The zero levels for the EM data are the voltage outputs of the inphase and quadrature channels in the absence of any secondary fields. Unlike time-domain systems, frequency-domain systems cannot turn off the primary field to determine the zero level. The typical procedure is to periodically fly the bird to a height well above the earth (200–300 m), so that measurable secondary fields cease to exist. There are a number of reasons why this procedure may not yield accurate zero levels at the usual survey altitude of 25–40 m; for example, a change in temperature with altitude can affect the transmitting-receiving coil separation or coil alignment. A 0.1-mm change in coil separation produces a response of the order of 40 ppm, whereas the goal is to have less than 2 ppm noise for the DIGHEM coil separation of 8.0 m. Additionally, the change in the ambient temperature at high altitude (during the system setup flying) from that at low altitude (during survey flying) may affect the zero levels of both the inphase and the quadrature. Thus, we may assume that the EM zero levels, obtained at high altitude, may need adjusting during low-level survey flying.

Parameters may also drift during low-level flying. Linear or nonlinear corrections to the zero levels may be required if, for example, the sun striking the bird varies due to clouds or to the EM system being flown back and forth in the typical grid pattern, as these can produce random or direction-dependent temperature fluctuations in the bird.

EM data are very altitude sensitive, with ppms varying approximately as the inverse cube of the sensor-source distance. When the EM system is flown to height, the rapid falloff of the EM signal with increasing height may cause the survey operator to conclude that the system has been raised beyond its detection limit of the earth and that the resulting receiving coil output reflects the true zero levels. If the ground is quite conductive, a few ppms may exist that are unnoticed by the operator or by the data processor. These few ppms will be lost, or zeroed out, during the data processing if care is not taken to recognize and rectify the problem. This error, if unrecognized, may cause a constant offset in the zero level or produce a tilt to the EM data. The resulting error in the computed resistivity, if not too severe, may be corrected with grid leveling techniques. In this paper, we assume that the initial EM zero leveling has been done on the inphase and quadrature channels. We describe certain grid leveling procedures which we use to eliminate or attenuate the residual resistivity leveling errors.

Half-space models for resistivity transformation

Because of the altitude sensitivity of an airborne EM system, a transformation should be performed on the EM data to yield an altitude-independent earth parameter to allow the EM survey to be useful for mapping. This is accomplished by use of a half-space model to transform helicopter EM data into resistivity. For soil salinity surveys, in contrast to mineral exploration, the data commonly are displayed as the conductivity rather than as its reciprocal, the resistivity.

Although a number of half-space models are available (Fraser, 1978), the so-called pseudo-layer half-space has become the model of choice for most helicopter EM operators. It is the only half-space model that does not use the flight height as an input, using only the inphase and quadrature channels (or, equivalently, the EM amplitude and phase) to compute the resistivity. Additionally, the dynamic range of the output resistivity is significantly greater than for the other half-space models.

LEVELING ERRORS IN AIRBORNE RESISTIVITY DATA

The resistivity, when gridded and imaged, typically indicates that some zero leveling errors in the inphase and quadrature data still exit. Rather than dealing with these directly by rezeroing the EM, we may choose to level the resistivity grid instead. In practice, resistivity leveling errors may be grouped into three types: leveling errors associated with a block of flight lines or an entire flight, leveling errors associated with flying direction, and a variety of leveling errors of smaller spatial wavelength.

Leveling errors associated with a block of flight lines

Leveling errors associated with a block of flight lines may be caused by the zero level of the EM channels being either too low or too high. Either of these conditions may cause the

earth to appear to be too conductive or too resistive, depending on whether the problem lies with the inphase or quadrature channel of a given frequency.

Flight-based leveling errors in the EM data may cause a broad constant offset in the resistivity of a block of flight lines. It is often easy to recognize this problem visually on the imaged resistivity map. The width of the affected block of flight lines usually varies from several hundred meters to several kilometers, depending on the survey. Figure 1a, having a north-south flight line direction, shows an example of this type of leveling error. The large conductive feature in the middle of the map is caused by an offset in the EM leveling. The constant offset causes the background resistivities in the block of lines to be lower than that of the surrounding flight lines.

If a pseudo tie-line is generated through a quiet (nonanomalous) area of this block (see line A-A′ of Figure 1a) and if the data on this pseudo tie-line are generated by sampling at each pseudo tie-line/flight-line intersection, then the data of the pseudo tie-line will mimic somewhat a square-wave form, as can be seen in the lower panel of Figure 1a. This type of leveling error can be handled by the semi-automated leveling technique described below.

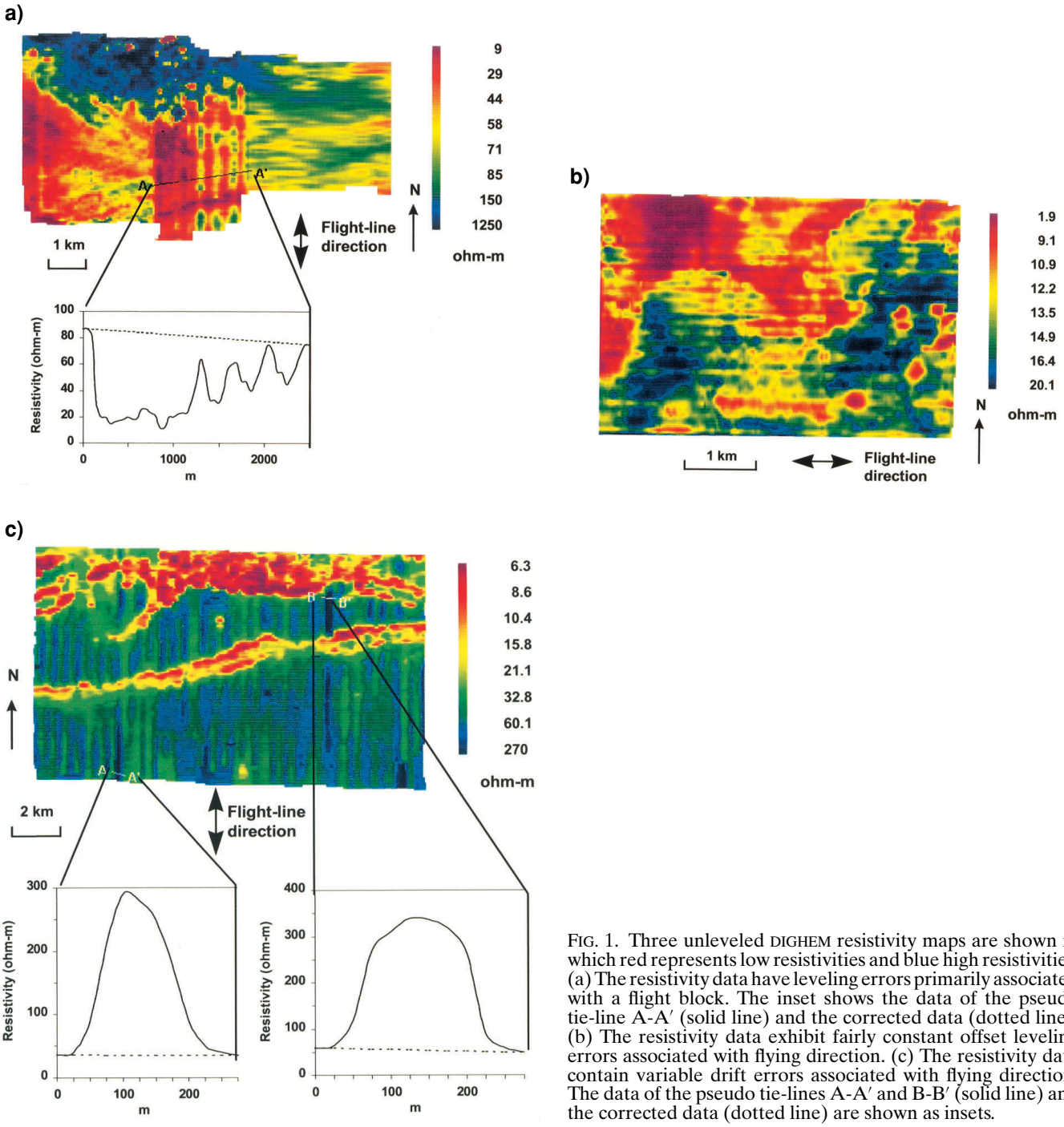

FIG. 1. Three unleveled DIGHEM resistivity maps are shown in which red represents low resistivities and blue high resistivities. (a) The resistivity data have leveling errors primarily associated with a flight block. The inset shows the data of the pseudo tie-line A-A′ (solid line) and the corrected data (dotted line). (b) The resistivity data exhibit fairly constant offset leveling errors associated with flying direction. (c) The resistivity data contain variable drift errors associated with flying direction. The data of the pseudo tie-lines A-A′ and B-B′ (solid line) and the corrected data (dotted line) are shown as insets.

Leveling errors associated with flying direction

The zero level of the EM data may change with every other flight line due to changes in flying direction. The amount of shift of the zero level on a flight line may either be primarily constant, as for the east-west flight lines of Figure 1b, or it may comprise a slow drift, as for the north-south flight lines of Figure 1c. In both cases, the leveling errors can be recognized by a striping pattern perpendicular to the flight lines. Some errors of this type also appear on the right half of A-A′ in Figure 1a.

If the constant offset or drift in the zero levels is not too serious, flight-line leveling errors can usually be removed by using the automated leveling method described below. Otherwise, the semi-automated leveling, based on some short pseudo tie-lines, should be applied first, as was done using A-A′ and B-B′ in Figure 1c.

Leveling errors of shorter spatial wavelength

In addition to the low-frequency flight-based and line-based leveling errors discussed above, there may be a number of minor leveling errors of a higher frequency due to instrument noise or inadequate semi-automated leveling corrections. These errors can also be removed by the automated leveling method.

RESISTIVITY LEVELING TECHNIQUES

The resistivity grid leveling procedures are performed in two steps. The first step, if necessary, employs semi-automated leveling using the pseudo tie-line leveling technique. This is used to remove any broad leveling errors caused by zero level errors in the EM data that may extend over blocks of flight lines. The method is also applicable to large leveling errors that affect a single line.

The second step employs an automated leveling technique based on a combination of nonlinear filters. This step rejects line-based resistivity leveling errors that yield striping image patterns and any remaining residual leveling errors. The basic methodologies used in the two steps are described below.

Semi-automated leveling

The primary purpose of the semi-automated leveling procedure is to remove the broad leveling errors, such as an offset or tilt, which may exist in a block of lines. This processing is done interactively by a geophysicist working with an imaged resistivity grid on a large computer screen. Such broad leveling errors can be recognized visually by examining the resistivity image (e.g., Figure 1a). A pseudo tie-line is then drawn with a mouse, more or less parallel to the geological strike, so that it crosses the block of flight lines to be leveled. The path selected for the pseudo tie-line should avoid areas of anomalous features and, if necessary, can be composed of a series of connected straight line segments. The two ends of the pseudo tie-line should be located in areas where the regional resistivity "background" is assumed to be correct.

The data on the pseudo tie-line can vary linearly or nonlinearly with distance, depending on the behavior of the regional or background resistivity. If the variation of the background resistivity along the pseudo tie-line is assumed to be approximately linear, the corrected data on this tie-line are obtained simply by linear interpolation between the two end points. An example is shown in the inset of Figure 1a. The corrected data of the tie-line represent the normal background and are used to remove resistivity leveling errors. The nonlinear lowpass filter described below is applied, parallel to the flight line direction, to the intersections of each line of cells and the pseudo tie-line before generating the pseudo tie-line data. This ensures that the pseudo tie-line data and the subsequent leveling corrections are not affected by local anomalous activity. The differences between the pseudo tie-line data and the corrected tie-line data are deemed to reflect the leveling errors for each line of cells in the block. These differences are subtracted from the lines of cells in the block being leveled. In this manner, the broad features due to flight block leveling errors are removed.

If a variation in the background resistivity along the pseudo tie-line is noticeably nonlinear, a different method has to be employed after the above lowpass filtering has yielded the pseudo tie-line data. The tie-line data can be represented as a function f(r) of distance r as shown in the example of Figure 2.

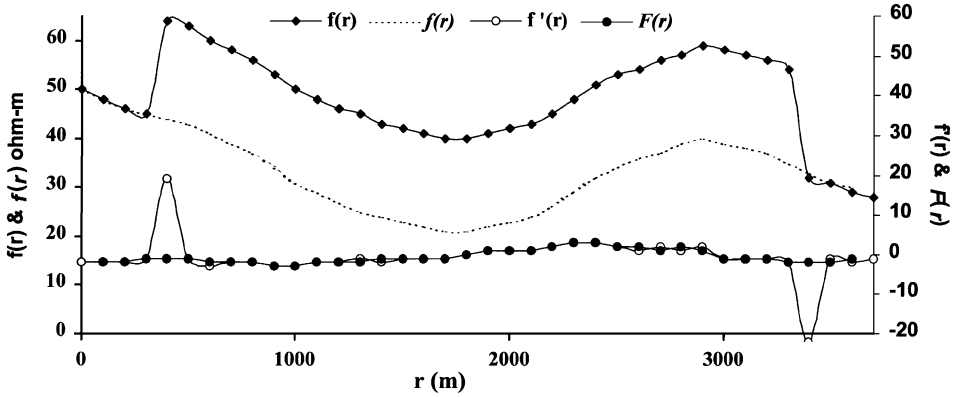

FIG. 2. This example of semi-automated leveling shows how offsets are handled for some data sets when the background resistivity data along the pseudo tie-line are not linear. f(r) is the resistivity data on the pseudo tie-line, f′(r) is the derivative of the pseudo tie-line resistivity data with respect to distance r, $F(r)$ is the result from a median filtering of f′(r), and $f(r)$ is the recovered resistivity data on the pseudo tie-line.

The offset represents the leveling error. Thus, the dashed line is deemed to be the true background; this is the curve we wish to obtain from our manipulation of the resistivity data.

The derivative $f'(r)$ of the pseudo tie-line data $f(r)$ is approximated by several delta functions showing where the resistivity curve jumps up and down. The derivative transforms the broad leveling error into the impulses shown or the derivative curve indicated by open circle symbols. These impulses may be significantly reduced by a nonlinear lowpass filter of appropriate length to yield the filtered curve identified by solid circle symbols. Then, an integration can be applied to the filtered derivative curve to yield the pseudo tie-line data without the offset.

The lowpass filtered result $F(r)$ can be written as,

$$F(r) = \mathrm{F}[\mathrm{f}'(r)]. \tag{1}$$

The integration of $F(r)$ yields the reconstructed function

$$f(r) = \int F(r)\,dr + C \tag{2}$$

where C is the integration constant equaling the value at the beginning of the pseudo tie-line. The dashed line is the reconstructed data. It represents a reasonable fit of the regional data along the pseudo tie-line. In practice, the integration may be obtained approximately by summation.

The differences between the reconstructed values and the original values on the pseudo tie-line are the corrections for the lines of cells crossing the pseudo tie-line.

If the resistivity leveling errors appear approximately as constant offsets, the corrections obtained by the above procedure can be subtracted from the lines of cells. If an approximate linear drift occurs, the whole line of cells can be tilted linearly. Tilting requires a second control point, which could be selected by a second pseudo tie-line. Alternatively, if the area needing correction is to be feathered into properly leveled data that exists along the line of cells (in the flight direction), the selected point must be free of a locally anomalous response. This point should be selected where the "roughness" of the data is at a minimum. The roughness R is given by

$$R = [(1/(N-1)] \sum_{i=1}^{N-1} (d_{i+1} - d_i)^2 \tag{3}$$

where N is the number of data points within a window, and d_{i+1} and d_i are the data. A search can be made along a line of cells by calculating the roughness in the direction perpendicular to the lines. The point with minimum roughness is selected as the second control point for tilting.

Automated leveling

After the low-frequency flight-based resistivity leveling errors and some large line-based leveling errors are removed by the semi-automated leveling, there may be some high-frequency across-line leveling errors which yield a striping appearance to the map images. These errors can be removed by one of a number of automated leveling methods. We have obtained satisfactory results by using a combination of 2-D and 1-D nonlinear median value-related filtering techniques. These are effective because the high-frequency across-line leveling errors tend to have the appearance of impulse noise. In particular, we prefer to use median filters (Regalia, 1993) or data-dependent nonlinear (DDNL) filters (Economou et al., 1995). A description of DDNL filters is presented in Appendix A. The median filter is much more efficient in the computation, whereas the DDNL filter yields smoother results for an operator of the same length and width.

Figure 3 shows a flow chart of the automated process, which involves several steps. First, a lowpass rectangular window filter (either a 2-D DDNL filter or a 2-D median filter), with its longer side perpendicular to the flight line direction, is employed on the input grid. Its output, which is the smooth background resistivity, is subtracted from the input to isolate the elongated leveling errors in the flight-line direction. The resulting interim output grid contains the leveling errors and some residual geological features. A 1-D lowpass filter (either a 1-D DDNL filter or a 1-D median filter) then is applied along the line direction of the interim output grid to reject the residual geological features, leaving only the leveling errors in the output error grid. Finally, the output error grid is subtracted from the input grid to yield the leveled resistivity grid.

The results from the automated leveling depend upon the size of the filter windows. The windows should be carefully chosen for a specific data set by examining the image of the data. If the rectangular 2-D filter window is too small, some leveling errors will be left in the results; if it is too large, the local background of the data may be shifted up or down incorrectly. If the 1-D filter length is too short, the amplitudes of some geological features will be reduced; if it is too long, some leveling errors with short wavelength will not be removed and edge effects may appear.

The automated leveling procedure is able to remove both long-and short-wavelength leveling errors, depending upon the size of the filter windows. In general, this leveling procedure

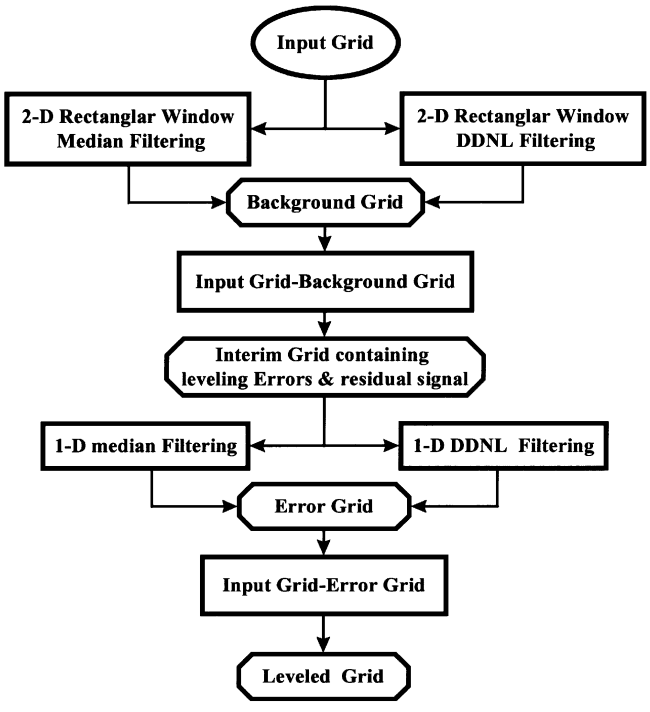

FIG. 3. Flow chart for the automated leveling procedure. The path follows either the median filtering or the DDNL filtering.

can be iterated several times if necessary to obtain an acceptable result. In practice, one pass is usually good enough for most data. Two passes may be needed for some data to remove different wavelength errors separately. If the wavelength of leveling errors is the same as that of geological features oriented parallel to the flight lines, the automated leveling method will not be able to distinguish between them. Therefore, it should be selectively applied.

Examples

The results of the leveling techniques for the poorly leveled examples of Figure 1 are shown in Figures 4–6.

Figure 4a shows the results of the semi-automated leveling, based on the pseudo tie-line A-A′ of Figure 1a. The major block leveling errors in the middle of Figure 1a have been removed by the semi-automated leveling, including the errors associated with flying direction on the right half of A-A′. Some features that were difficult to see on the original map of Figure 1a have been significantly enhanced. The continuity of linear features that strike at an oblique angle to the flight lines has also been improved. However, there still remains a line-based resistivity high on the far left side of Figure 4a, as well as other minor leveling errors including errors produced by inadequate or excessive semi-automated leveling.

The semi-automated leveled data of Figure 4a becomes the input to the automated leveling procedure, the output of which is shown in Figure 4b. All geological details appearing on the original map of Figure 1a remain in Figure 4b, and all observed leveling errors are removed. The error grid of Figure 4c is computed as the difference between the logarithms of the resistivities of the input and output grids, which is equivalent to the ratio of the original resistivity to the corrected resistivity (see color bar). Figure 4c does not appear to contain any geological

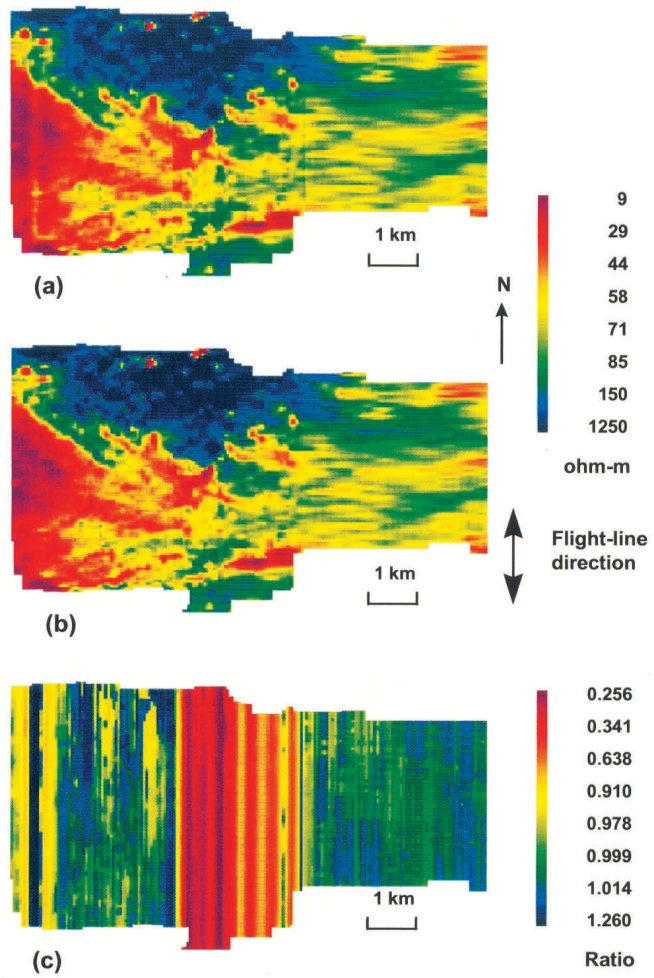

FIG. 4. The results of applying the leveling procedures to the resistivity data of Figure 1a are shown after (a) semi-automated leveling, which is then followed by (b) automated leveling. The errors (c) removed through the two leveling steps do not indicate that any significant geological signal has been removed. The color bar in Figure 4c shows the ratio of the original resistivity to the corrected resistivity.

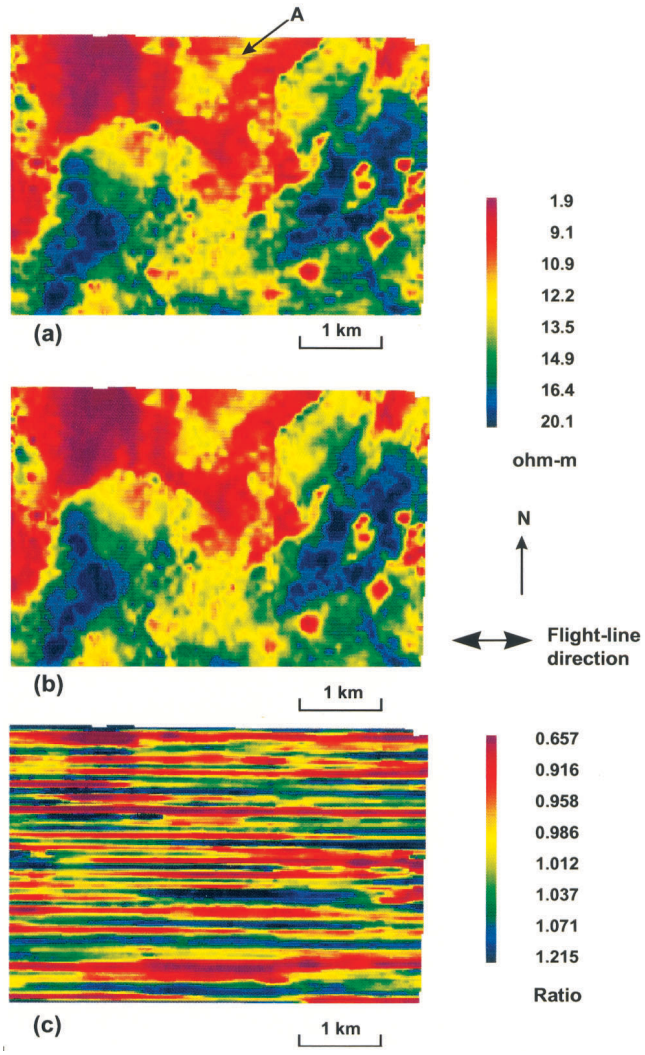

FIG. 5. The leveling results are presented for the input resistivity grid of Figure 1b. (a) This map results from the automated leveling using large filter windows. (b) The output of Figure 4a is then used as input to another automated leveling with smaller filter windows. (c) The errors removed through the two leveling steps do not indicate a loss of geological information. The color bar in Figure 5c shows the ratio of the original resistivity to the corrected resistivity.

signal, implying that geological information was not noticeably impaired by the leveling operations.

Figure 5 shows the results of the leveling methods for the data of Figure 1b. The automated leveling method was the only technique applied to the data in Figure 1b because it is powerful enough to handle striping errors like this. The automated leveling procedure was iterated twice. This data set has 198 × 179 cells. Relatively large filter windows (25 × 5 cells for the 2-D filter and 71 cells for the 1-D filter) were used in the first pass to remove the long-wavelength line-based leveling errors. The resulting output data are shown in Figure 5a. It can be seen that the long wavelength line-based leveling errors are fairly well removed. However, some minor high frequency errors are left, as can be recognized by some short elognated features along the flying direction (e.g., at point A in Figure 5a). A second pass with smaller filter windows (7 × 5 cells for the 2-D filter and 31 cells for the 1-D filter) was applied to the results from the first pass. The final result, shown in Figure 5b, is relatively free of the minor leveling errors. The imaged error grid containing all the deleted leveling errors is shown in Figure 5c, and appears to be free of geological signal.

For the data in Figure 1c, semi-automated leveling was applied using pseudo tie-lines A-A′ and B-B′ to correct two seriously misleveled narrow blocks of cells. This produced Figure 6a, which itself served as the input to the automated leveling procedure, yielding Figure 6b. It can be seen from this figure that the striping features have been removed and the quality of the data has been substantially improved. The error grid of Figure 6c appears to be free of geological signal.

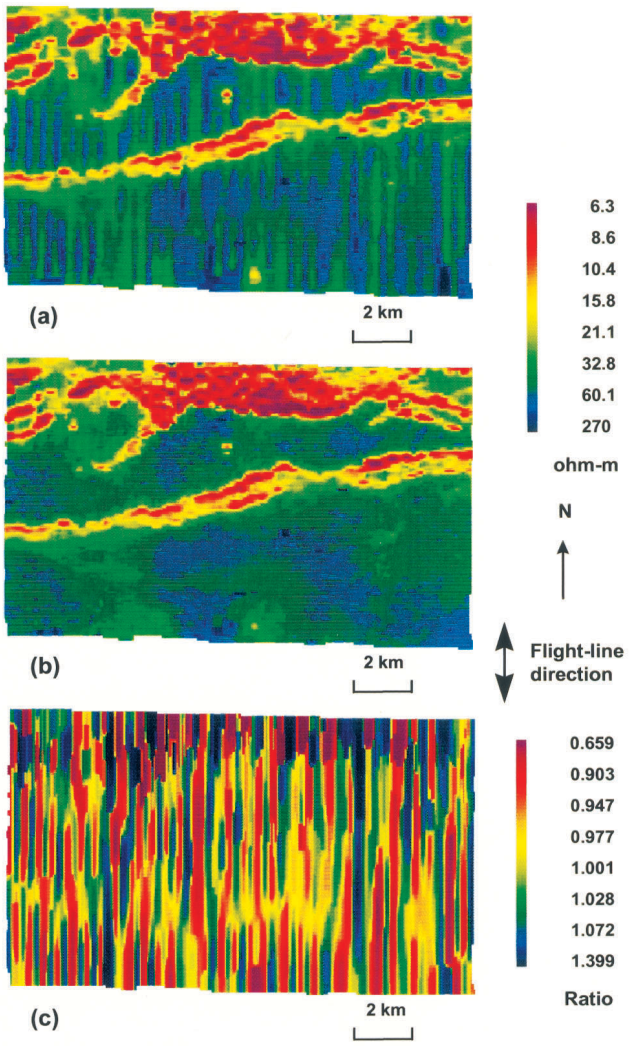

FIG. 6. The leveling results for the map of Figure 1c show the data after (a) semi-automated level tilting followed by (b) automated leveling. The removed leveling errors (c) show the ratio of the original resistivity to the corrected resistivity. The error grid suggests that no significant geological signal has been removed.

CONCLUSIONS

The integrity of the resistivity data obtained from helicopter-borne electromagnetic surveys depends critically on the processing techniques and is particularly governed by the leveling procedures. Poor leveling procedures may in fact generate false resistivity features as well as eliminate real ones. Consequently, it behooves the user to be aware of the leveling techniques used to produce the resistivity maps.

Semi-automated and automated grid leveling procedures may be used to produce resistivity maps that maintain the integrity of the data while enhancing geological features and improving the appearance of the resistivity maps. There are many ways to accomplish this using 1-D and 2-D filtering techniques. The semi-automated pseudo tie-line approach and the automated use of median and data dependent nonlinear filters appears to work quite well for the DIGHEM helicopter EM survey data shown in the above examples.

The semi-automated leveling method uses pseudo tie-lines to remove the broad features caused by leveling errors in a block of flight lines and any high-magnitude line-based errors. An automated leveling method uses a combination of 1-D and 2-D nonlinear filters to reject all remaining errors, including both long-and short-wavelength leveling errors. The automated method must be used with care because it cannot distinguish between leveling errors and geological features with similar wavelengths that are parallel to the flight lines.

The leveling procedures are applied to the resistivity grid after the inphase and quadrature EM channels in the database are themselves zero leveled. The zero leveling of the EM channels is imperfect, which is why the grid leveling of the resistivity is needed. The issue then arises as to whether the leveling of the EM channels can be adjusted to reflect the final resistivity grid. Such adjustments may be possible by solving for the EM response based on the resistivity data in the absence of anomalous features. The difference in the computed and measured EM values then could be used to adjust the EM channel leveling. If the process were done correctly, the adjusted EM channels, when transformed, would yield the same resistivity as that obtained by the grid leveling of the resistivity without loss of the high-frequency fidelity of the EM data. The usefulness of this approach is currently being evalauted.

ACKNOWLEDGMENTS

We thank Dr. Richard Smith and Dr. Peter Wolfgram of Geoterrex-Dighem for their comments on this paper. Appreciation is expressed to Geoterrex-Dighem for permission to publish.

REFERENCES

Becker, A., 1988, Airborne resistivity mapping: IEEE Trans. on Antennas and Propagation, **36**, 557–562.

Deletie, P., and Lakshmanan, J., 1986, Airborne resistivity surveying applied to nuclear power plant site investigation in France, *in* Palacky, G. J., Ed., Airborne resistivity mapping: Geol. Surv. Canada Paper 86-22, 145–152.

Dyck, A. V., Becker, A., and Collet, L. S., 1974, Surficial conductivity mapping with the airborne INPUT system: Can. Inst. Min. Metallurg. Bull., **67**, 104–109.

Economou, G., Fotopoulos, S., and Vemis, M., 1995, A family of nonlinear filters with data dependent coefficients: IEEE Trans. on Signal Processing, **43**, 318–322.

Fitterman, D. V., and Deszcz-Pan, M., 1998, Helicopter EM mapping of saltwater intrusion in Everglades National Park, Florida: Explor. Geophys., **29**, no. 1/2, 240–243.

Fraser, D. C., 1978, Resistivity mapping with an airborne multicoil electromagnetic system: Geophysics, **43**, 144–172.

——— 1979, The multicoil II airborne electromagnetic system: Geophysics, **44**, 1367–1394.

Hasegawa, K., Davidson, G. I., Wollenburg, P., and Iida, Y., 1990, Geophysical exploration for unconformity-related uranium deposits in the northeastern part of the Thelon Basin, Northwest Territories, Canada: Mining Geol., **40**, 83–95.

Hoover, D. B., and Pierce, H. A., 1986, Airborne electromagnetic mapping of geothermal systems in the Basin and Range and Cascade provinces, U.S.A., *in* Palacky, G. J., Ed., Airborne resistivity mapping: Geol. Surv. Canada Paper 86-22, 99–106.

Huang, H., and Fraser, D. C., 1996, The differential parameter method for multifrequency airborne resistivity mapping: Geophysics, **61**, 100–109.

James, D. R., 1992, Lac de Gras, Northwest Territories, diamond exploration play: Richardson Greenshields Equity Research, no. 92-215.

Regalia, P. A., 1993, Special filter designs, *in* Mitra, S. K., and Kaiser, J. F., Eds., Handbook for digital signal processing: John Wiley & Sons, Inc., 907–980.

Sengpiel, K. P., 1986, Groundwater prospecting by multifrequency airborne electromagnetic techniques, *in* Palacky, G. J., Ed., Airborne resistivity mapping: Geol. Surv. Canada Paper 86-22, 131–138.

Soonawala, N. M., and Hayles, J. G., 1986, Airborne electromagnetic methods in the concept assessment phase of the Canadian nuclear fuel waste management program, *in* Palacky, G. J., Ed., Airborne resistivity mapping: Geol. Surv. Canada Paper 86-22, 153–158.

Taylor, S., 1990, Airborne EM resistivity applied to exploration for disseminated precious metal deposits: The Leading Edge, **7**, no. 2, 34–41.

Won, I. J., and Smits, K., 1986, Application of the airborne electromagnetic method for bathymetric charting in shallow ocean, *in* Palacky, G. J., Ed., Airborne resistivity mapping: Geol. Surv. Canada Paper 86-22, 99–106.

APPENDIX A

DATA DEPENDENT NONLINEAR FILTERS

The DDNL filters are a family of data dependent nonlinear filters. The coefficients of a DDNL filter are computed locally, and the absolute difference between data is used to determine a rank-order-dependent weighting function. The filters were developed originally as 1-D filters (Economou et al., 1995). However, the coefficient of the filters at a certain datum point depends only upon the absolute difference between the datum and all data in the filter window rather than upon its position in the window. Therefore, the 1-D DDNL filter can be extended to 2-D filters as shown following.

Let **d** be the 2-D vector of $L = M \times N$ data,

$$\mathbf{d} = \{d_{ij}\}, \quad i = 1, 2, \ldots, M; \quad j = 1, 2, \ldots, N. \quad \text{(A-1)}$$

Then, a $L \times L$ matrix **A** can be defined over **d**. Its $(j-1) \times N + i$th row contains the absolute differences between d_{ij} and all elements of **d**. Matrix **A** contains all the information concerning the absolute differences between data points. It is a $L \times L$ symmetric matrix with a zero diagonal.

The vector $\mathbf{L} = [\ell_l \ldots \ell_L]^T$ is defined as the product

$$\mathbf{L} = \mathbf{A}\,\mathbf{I}, \quad \text{(A-2)}$$

where **I** is the unit vector of length L and T is the transpose operation. Each element $\ell_{(j-1)\times N+i}$ of the vector **L** is equal to the sum of the absolute differences of d_{ij} to all the other data points within **d**. Of course, **L** has a minimum value element ℓ_m,

$$\ell_m = \sum_{i=1}^{M} \sum_{j=1}^{N} |d_m - d_{ij}|, \quad \text{(A-3)}$$

where d_m is the median value of the elements in the vector **d**. Also the value of $\ell_{(j-1)\times N+i}$ increases according to the difference of d_{ij} from the median. A new vector **C** with elements that are a function of the elements of **L** can be defined as

$$c_{(j-1)\times N+i} = f\left(\ell_{(j-1)\times N+i}\right)$$

$$i = 1, \ldots, M \quad \text{and} \quad J = 1, \ldots, N. \quad \text{(A-4)}$$

These are the coefficients of the new filter. When polynomial relations are used, the following filter families can be defined as

$$c_{(j-1)\times N+i} = 1 \Big/ \ell^{p}_{(j-1)\times N+i} \qquad p = 1, 2, 3 \ldots \quad \text{(A-5)}$$

As the power of p is increased, the weighting function of the filter becomes more peaked at the median value. Having the coefficients $c_{(j-1)\times N+i}$ in equation (A-5), the output value d of the data dependent nonlinear filter is computed by

$$d = \sum_{i=1}^{M} \sum_{j=1}^{N} c_{(j-1)\times N+i}\; d_{ij} \Bigg/ \sum_{i=1}^{M} \sum_{j=1}^{N} c_{(j-1)\times N+i}. \quad \text{(A-6)}$$